J Sol-Gel Sci Technol (2011) 59:174–180
DOI 10.1007/s10971-011-2478-8

ORIGINAL PAPER

Effect of synthesis conditions on the microstructure of TEOS derived silica hydrogels synthesized by the alcohol-free sol–gel route

Mercedes Perullini · Matías Jobbágy · Sara A. Bilmes · Iris L. Torriani · Roberto Candal

Received: 8 February 2011 / Accepted: 28 April 2011 / Published online: 12 May 2011

Abstract Silica matrices synthesized from a pre-hydrolysis step in ethanol followed by alcohol removal at low pressure distillation, and condensation in water, are suitable for encapsulation of biomolecules and microorganisms and building bioactive materials with optimized optical properties. Here we analyze the microstructure of these hydrogels from the dependence of *I(q)* data acquired from SAXS experiments over a wide range of silica concentration and pH employed in the condensation step. From the resulting data it is shown that there is a clear correlation between the microscopic parameters—cluster fractal dimension (*D*), elementary particle radius (*a*) and cluster gyration radius (*R*)—with the attenuation of visible light when the condensation step proceeds at pH < 6. At higher pHs, there is a steep dependence of the cluster density ($\sim R^{D-3}$) with the condensation pH, and non-monotonous changes of attenuance are less than 20%, revealing the complexity of the system. These results, which were obtained for a wide pH and silica concentration range, reinforce the idea that the behavior of gels determined in a restricted interval of synthesis variables cannot be extrapolated, and comparison of gelation times is not enough for predicting their properties.

Keywords Silica hydrogels · TEOS alcohol-free · SAXS microstructure characterization · Optical quality

1 Introduction

Sol–gel process is a well known route for the synthesis of novel inorganic and hybrid materials ranging from ceramics to biocompatible soft inorganic gels. The properties of the final product can be tuned by controlling the solution parameters from which a sol and a particulate or polymeric network are formed [1]. Silica based hydrogels are recognized as suitable matrices for building hybrid materials with biological activity by encapsulation of enzymes, antibodies or other macromolecules [2–4]. Moreover, stable and non-degradable silica-based hydrogels are extensively used for living cells entrapment [5–7] for different applications, such as the design of biosensors [8] or modular bioreactors [9, 10].

The encapsulation of living cells inside inorganic matrices implies an intrinsic limitation in synthesis conditions, as the overall process must evolve within biocompatible chemical constraints imposed by the encapsulated cell strain [11]. On the other hand, depending on the application for which the biomaterial is developed, some macroscopic properties of such wet gels are desirable or even necessary. Examples of these cases are biosensors and devices based on encapsulation of photosynthetic cells in which the optical properties are of crucial importance

Electronic supplementary material The online version of this article (doi:10.1007/s10971-011-2478-8) contains supplementary material, which is available to authorized users.

M. Perullini (✉) · M. Jobbágy · S. A. Bilmes · R. Candal (✉)
INQUIMAE-DQIAQF, Facultad de Ciencias Exactas y Naturales, Universidad de Buenos Aires, Ciudad Universitaria, Pab. II, C1428EHA Buenos Aires, Argentina
e-mail: mercedesp@qi.fcen.uba.ar

R. Candal
e-mail: rjcandal@qi.fcen.uba.ar

R. Candal
ECyT, Universidad Nacional de San Martín, Campus Miguelete, San Martín, Buenos Aires, Argentina

I. L. Torriani
Institute of Physics Gleb Wataghin, State University of Campinas, Campinas, SP, Brazil

[12, 13]. In these cases, the optimization of optical quality must fulfill other needs, such as porosity, density, hardness and elasticity that require a fine control of the synthesis parameters and a detailed characterization of their structure in the 0.1 nm–1 μm range. Nevertheless, the achievement of materials with good macroscopic properties often produces death or stress due to the release of toxic by-products originated during the synthesis [14]. Nowadays a wide range of potential applications are envisaged which demand a growing variety of strains and the development of novel host materials and/or synthetic pathways is necessary to satisfy particular requirements.

The relationship between synthesis parameters, microstructure and macroscopic properties is still a challenge for the design of hybrid and bioactive materials based on silica derived from sol–gel pathways. During the last decades, the bulk structure of silica based gels has been extensively studied mainly by scattering techniques (neutrons, X-ray, light) [15–17]. It has been shown that the silica backbone is formed by fractal clusters resulting from condensation and particle-aggregation processes [18, 19]. These clusters can be described by their radius of gyration (R), the radius of gyration of the elementary particles composing the cluster (a) and their fractal dimension (D)[1] that represents de mass distribution in the volume: m–r^D, where m is the mass and r is the distance in the D-dimensional space [20]. It was found that the fractal dimension (D) ranges between 2.2 and 1.7 [21] depending on the gelation mechanism, e.g. Diffusion Limited (DLA) or Reaction Limited (RLA) cluster–cluster Aggregation [22, 23].

Although one common pathway for SiO_2 gel formation is the catalytic polycondensation of tetra-alkoxysilanes in an alcoholic environment [24–26], cytocompatible silica hydrogels are mainly synthesized from aqueous sodium silicates [27–31], where the harmfulness of the alcohol by-product is avoided at the expense of the osmotic stress produced by Na^+ ions [14, 32]. These aqueous derived gels usually exhibit poorer optical and mechanical properties than those synthesized in alcohol. Another way to enhance the viability of encapsulated cells using the alcoxide route is to separate the hydrolysis and condensation steps. Hydrolysis is performed in acid media with water added as a limiting reagent, followed by low pressure removal of the cytotoxic alcohol [33–35]. In this alcohol-free route, for building bioactive materials, the condensation of alkoxide precursors is done immediately before the addition of living cells suspended in a buffer aqueous solution at the appropriate physiological pH. Thus, although the hydrolysis is conducted in alcohol, the aggregation and condensation processes occur in aqueous media, and the resulting hydrogels display distinct macroscopic properties.

Within this framework, the aim of this work is to establish a correlation between the microstructure and macroscopic properties—such as optical quality—in order to rationalize the synthesis of alcohol-free tetraethoxysilane derived silica hydrogels (AFTD) for the design of bioactive materials. The approach employed to achieve this goal is the analysis of the scattering function, $I(q)$, obtained from SAXS experiments for silica hydrogels with variable concentration of silica and condensation pH. From the obtained results, two regions with different behavior are defined in relation to the dependence of microstructure and optical quality with the synthesis conditions.

2 Materials and methods

Different parameters such as the condensation pH and the concentration of silica precursors were systematically changed, thus controlling time of gelation and structure of the formed hydrogel. TEOS (Aldrich) was employed as silica precursor, following the alcohol free procedure [33]. Briefly, a silica sol stock solution was prepared by mixing 5.58 mL of tetraethoxysilane (TEOS, from Sigma–Aldrich), 1.9 mL of water and 0.125 mL of HCl 0.62 M. The mixture was stirred vigorously to obtain a homogeneous solution (i.e. to completeness of the hydrolysis reaction). The removal of the alcohol (up to ≈96%) was achieved by rotavapor with controlled vacuum (30 mbar) and soft thermal treating (40 °C) on the hydrolyzed and diluted sol (50% in water). Different volumes of silica sol stock and phosphate buffer solutions (0.1 M, pH between 6 and 8) were mixed to obtain silica content between 3.6 and 10.7% in the final hydrogel samples, condensed at pH between 2.5 and 7.5.

The optical properties were evaluated by attenuance at 400 nm of samples aged 24 h in phosphate buffer (pH 6.5, 0.1 M).

The microstructure characterization was performed at the LNLS SAXS2 beamline in Campinas, Brazil, working at $\lambda = 0.1488$ nm, wave vector range: $0.09\ \text{nm}^{-1} < q < 2.2\ \text{nm}^{-1}$ and a sample stage in vacuum with mica windows (standard for liquids) [36]. Data analysis was done with SASfit program [37].

3 Results

Figure 1 shows the evolution of the gelation time (t_g) with silica concentration and the pH at which condensation occurs. The hydrolysis conditions were identical for all the prepared samples while the pH of condensation was varied from 2.5 to 7.5. For all silica concentrations used in this

[1] As discussed later, in the Sect. 3, the interpretation of experimental results as indicating "fractality" is a matter of discussion (see Vinogradova et al. [39]).

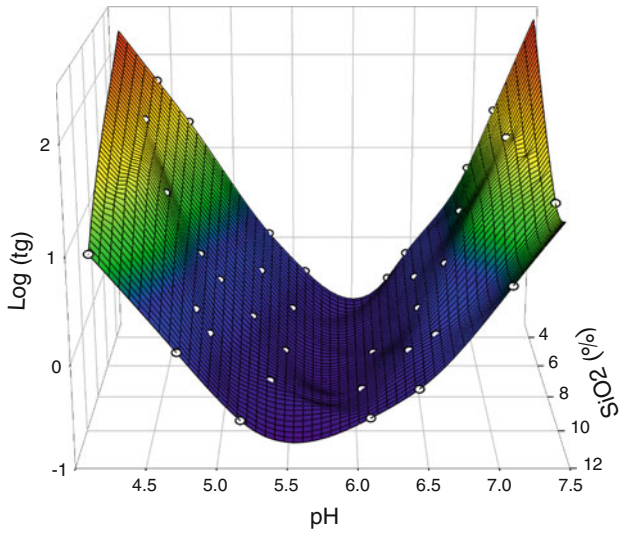

Fig. 1 Logarithm of the gelation time, t_g (in minutes), determined for hydrogels as a function of silica concentrations and pH of condensation. The *symbols* correspond to the experimental measurements

work, the gelation time presents a minimum in the pH range 5.5–6.0 (pH_{min}). It is worth noting that although the dependence of gelation time with pH follows the same trend for different silica concentrations, increasing the amount of silica causes a shift of the pH_{min} towards lower pH values.

Figure 2 shows plots of the SAXS intensity *I(q)* as a function of the modulus of scattering vector, q, for the hydrogels with different silica content (3.6–10.7%), synthesized at different condensation pH (2.5–7.5). The log–log SAXS intensity plots of AFTD hydrogels can be modelled as a mass fractal system [18, 19, 38, 39], although the rigorous interpretation of experimental results as indicating "fractality" requires many orders of magnitude of power-law scaling [40]. In this work, as the empirical values of D fall in the fractal regime $0 < D < 3$, the parameter D will be denoted as "fractal dimension", allowing a comparison between the experimentally derived objects and simulated objects obtained from fractal models.

Figure 3 show the different fitting parameters of the scattering curves: the radius of gyration of the elementary units, the fractal dimension and the radius of gyration of the primary cluster, respectively, as a function of the condensation pH for different SiO_2 concentration.

The fractal dimension (D) and the radius of gyration of the primary cluster (R) were evaluated in terms of a mass fractal aggregation model, with an autocorrelation function of the form

$$g(r) \approx r^{D-d} h(r, \xi)$$

where d is the spatial dimension and the exponential cut-off function h describes the perimeter of the aggregate [41]. The parameter ξ is a cut-off length for the fractal correlation, proportional to the radius of gyration (R).

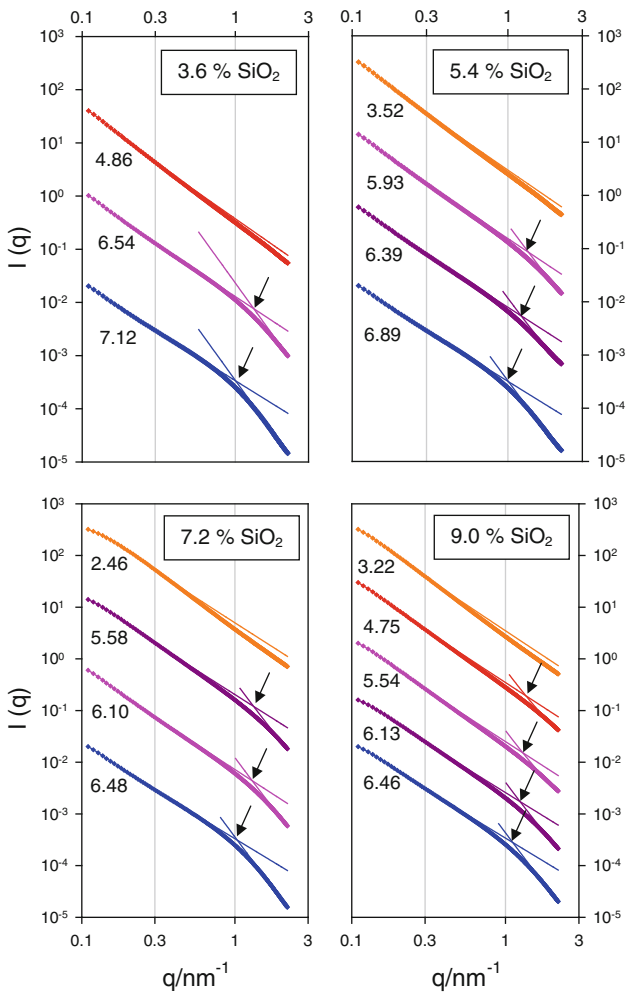

Fig. 2 Log-log SAXS intensity plots of TEOS derived hydrogels at the pH values indicated on each curve. The *fine-lines* are fittings of the experimental data using the mass fractal approach (*low q region*) and the power law at the Porod region (*high q region*). The curves are vertically shifted for clarity. The *arrows* show the q values from which the radius of gyration of elementary particles, *a,* is derived

$$h = \exp\left[-\frac{r}{\xi}\right]$$

$$\xi^2 = \frac{2R^2}{D(D+1)}$$

The values of the parameter a are obtained from the scattering curves from the q value corresponding to the intersection of the fit calculated for the experimental curve with the mass fractal approximation and the linear fit of the Porod region (indicated by the arrows in Fig. 2). The fact that for higher values of q the scattering curves can be fitted by the Porod approximation, $I(q) \sim q^{-4}$, indicate that we are dealing with Euclidean elementary particles (i.e. dense particles) instead of polymeric clusters of radius a.

Both R and D (Fig. 3a, b) show a slight dependence on pH below pH $\sim$ 5.5 and a steepest variation above this pH

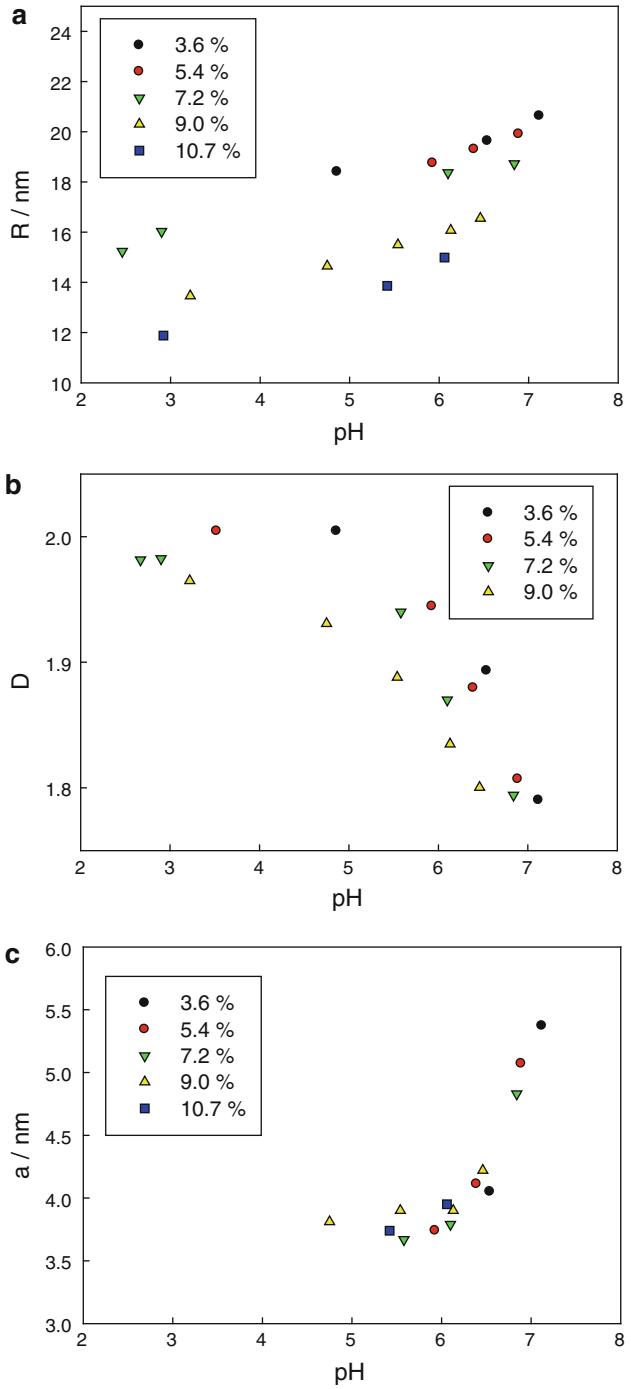

Fig. 3 Parameters derived from the fit of scattering curves as those in Fig. 2 as a function of condensation pH for the silica concentration indicated in the legends. **a** *R* Radius of gyration of primary clusters, **b** *D* Fractal dimension, **c** *a* Radius of gyration of the elementary particles

value, and decrease as the silica concentration increases (see Supplementary Information, figures SI-2 and SI-3).

As can be seen in Fig. 3c, the parameter *a* is strongly dependent on the condensation pH but it is independent of the silica concentration, as all the compositions fall in the same curve. At pH values below 4.5, no dense particles can be observed in the *q* range studied (i.e. with a radius of gyration >3 nm).

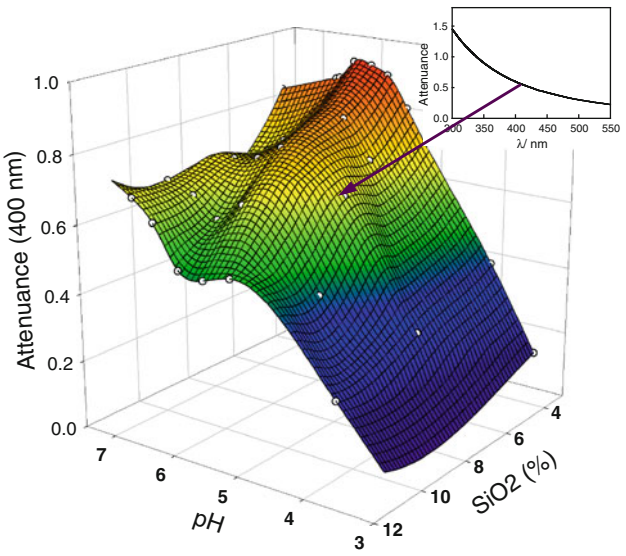

Fig. 4 Attenuance at 400 nm of hydrogels as a function of the silica concentration and the condensation pH. The *symbols* correspond to the experimental measurements. *Inset* UV–vis spectra of one representative sample (silica content of 7.2%, condensation pH = 5.13); the corresponding data point is shown by the *arrow*

Figure 4 shows the dependence of the attenuance at 400 nm of AFTD hydrogels with silica concentration and the pH of condensation. As a general trend, for a fixed silica concentration, the attenuance increases with the condensation pH, presenting a relative maximum at a pH ∼ 6. It is worth noting that this pH value coincides with the pH of the minimum gelation time (pH_{min}) for each silica concentration (see Fig. 1). For samples synthesized at a fixed condensation pH in the range 3–6, raising the silica concentration improves their optical quality. However, for higher pH values, the attenuance does not follow a simple trend with respect to the condensation pH and/or the silica concentration.

4 Discussion

The polymerization of alkoxysilanes leading to gels involves hydrolysis and condensation reactions. In this particular case both stages can be differentiated because condensation is negligible in acid media at which hydrolysis is conducted [1]. In contrast, the condensation is catalysed by OH^- and thus it goes faster at higher pH. From a macroscopic point of view, hydrolysed species can condense to form dense silica particles statistically distributed in the sample volume, which in turn diffuse and aggregate to form the fractal clusters that collide to form a

gel (see Supplementary Information figure SI-1). The attachment of particles to form clusters and cluster–cluster aggregation to form larger structures is also dependent on the pH of the condensation stage. Since the surface of silica is negatively charged above the isoelectric point, the higher the pH, the stronger the electrostatic repulsion between the particles (see Supplementary Information figure SI-3).

For all the silica concentrations used in this work, the gelation time presents a minimum in the pH range 5.5–6.0. At a higher pH, aggregation is impeded by particle charge and, on the other hand, at lower pH, basic catalysis is inhibited by $[H^+]$. Similar results were observed for the gelation of silica in aqueous media from sodium silicate solutions [42]. The shift of pH_{min} to lower values as the silica concentration increases reveals a compromise between condensation rate and the electrostatic repulsion between the particles and/or clusters. Increasing silica concentration contributes to a faster condensation rate, but does not modify the electrostatic repulsion. The latter being dependent on the pH, and in consequence the maximum gelation rate is attained at a lower pH for a higher silica concentration.

The dependence of a with pH (Fig. 3c) puts on evidence that the elementary particles are not those formed during pre-hydrolisis [43]. Their increase in size with the pH (Fig. 3c) is attributable to the higher solubility of silica in water as the pH increases and the growing of these basic units by Ostwald ripening [1]. The fractal dimension decreases from an initial value of 2.0 at low pH, to 1.8 at high pH. Essentially the same results were reported for the condensation of tetra-alkoxysilanes in alcoholic medium and for particle aggregation in sodium silicate solutions [24, 31]. A fractal dimension of 2.0 is close to the value found for reaction limited cluster–cluster aggregation (2.1–2.2) [21]. At low pH the rate of condensation is low and particles link mainly by hydrogen bonds. As inter-particle repulsion is negligible and elementary particles are not linked by covalent bonds, rearrangements by which particles of the periphery are released to stick to the inner part of the cluster give as a result smaller and denser structures (i.e. with a higher fractal dimension). On the other hand, a fractal dimension of 1.8 is close to the value found for diffusion limited cluster–cluster aggregation (1.75–1.80) [21]. When the condensation rate is high, the contact between particles results in an irreversible connection by covalent bonding. Most collisions yield growth of the aggregates, so that the overall growth rate approaches that of the diffusive flux. As covalent bonds do not easily break up, rearrangements are not frequent and the growing of clusters occurs in the periphery due to inter-particle repulsion. This gives less dense structures with a higher radius of gyration. As shown in Fig. 3a and b, the pH value at which the system changes from one regime to the other depends on the silica concentration and coincides with the pH_{min}.

Contrary to what was found for aqueous silicate aggregation systems that employ sodium silicates as precursors, [44, 45] AFTD hydrogels synthesized at a condensation pH between 3 and 6, show a lower attenuance (e. g. better optical quality) for a higher silica concentration (Fig. 4). The spectra of all AFTD hydrogels (one example is shown in the inset of Fig. 4), exhibit lower attenuance at higher wavelength, according to the Rayleigh relation [46].

$$\frac{I}{I_0} = A \exp\left(-B\frac{r^3}{\lambda^4}\right)$$

where r is the radius of the scattering particles and λ is the wavelength of the incident light. It is worth noting that the Rayleigh relation is defined for isolated and mono-dispersed particles at low concentration. In these gels, all the clusters contributing to the light scattering include the first-generation clusters (characterized by parameters R and D) and higher-order generation clusters composing the gel structure (see Supplementary Information, figure SI-1). It is important to point out that the size of the elementary units characterized by the parameter a is too small to generate a significant scattering in the UV–vis range. From the correlation between the attenuance and R shown in Fig. 5 it can be concluded that below pH_{min} the optical quality is given by the first generation clusters. For higher pH values, the attenuance does not follow a simple trend with respect to the condensation pH or the silica concentration.

The differences in the behaviour below and above pH_{min} are possibly related to the density of the aggregates. For a fractal body, the density is proportional to the mass ($\sim R^D$) to volume ($\sim R^3$) ratio. As seen in Fig. 6, the density of the

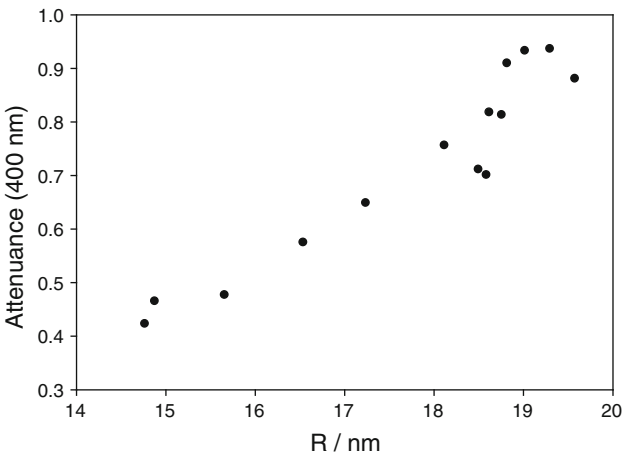

Fig. 5 Attenuance at 400 nm of AFTD hydrogels synthesized at different condensation pH (3–6) versus Radius of gyration of the primary cluster (R) as derived from SAXS experiments

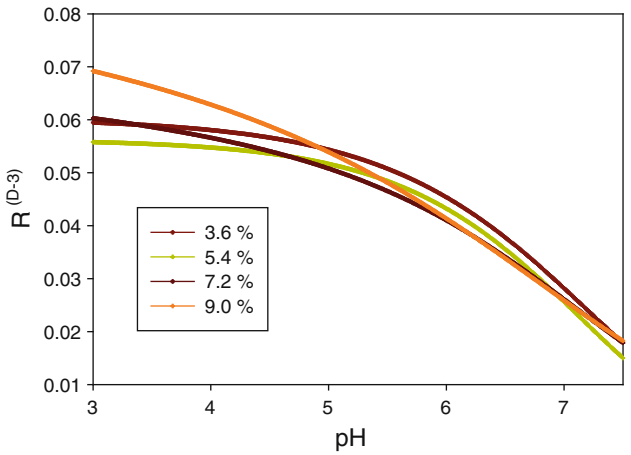

Fig. 6 Cluster density, $R^{(D-3)}$, as a function of condensation pH for AFTD hydrogels with different silica concentrations, indicated in the legends

clusters is nearly constant below pH_{min}, and decreases for higher pH values.

5 Conclusions

The SAXS characterization of the microstructure presented here provides a rational basis to select the appropriate synthesis conditions to fulfil requirements of particular applications, with special emphasis on those which demand good optical properties. For AFTD hydrogels presented here, in the pH range below the pH of the minimum gelation time (pH_{min}) there is a good correlation between the optical quality and their microstructure. In this pH region there are slight variations of the microstructural parameters with pH, whereas the attenuance exhibits a monotonous increase with pH up to nearly one order of magnitude. Above pH_{min}, the microstructure is very sensitive to the condensation pH whereas the attenuance has a slow and non-monotonous pH dependence. The density of primary clusters in these two regions also exhibits a different behaviour: it is nearly constant below pH_{min}, and decreases with pH above this pH value. Our results obtained in a wide pH and silica concentration range reinforce the idea that the behavior of gels determined in a restricted range of synthesis variables can not be extrapolated, and comparison of gelation times is not enough for predicting properties.

This approach should contribute to the design of a rational synthesis pathway for different applications, and in particular, for bio-applications where the compatible pH range is close to the pH_{min}.

Acknowledgements This work has been supported by the Brazilian Synchrotron Light Laboratory (LNLS, Brazil, proposal D11A-SAXS-6039), the scientific collaboration agreement CAPES-SECyT (Brazil-Argentina, 011/02), the University of Buenos Aires (UBACyT X-003), and by National Research Council of Argentina (CONICET PIP 11220080102533). SAB, RC, MJ and MP are Research Scientists of CONICET (Argentina).

References

1. Brinker CJ, Scherer G (1990) Sol gel science. Academic Press, San Diego
2. Gill I, Ballesteros A (1998) Encapsulation of biologicals within silicate, siloxane, and hybrid sol–gel polymers: an efficient and generic approach. J Am Chem Soc 120(34):8587–8598
3. Avnir D, Brown S, Lev O, Ottolenghi M (1994) Enzymes and other proteins entrapped in sol–gel materials. Chem Mater 6(10):1605–1614
4. Avnir D, Lev O, Livage J (2006) Recent bio-applications of sol-gel materials. J Mater Chem 16(11):1013–1030
5. Livage J, Coradin T (2006) Living cells in oxide glasses. Rev Mineral Geochem 64(1):315–332
6. Soltmann U, Böttcher H (2008) Utilization of sol-gel ceramics for the immobilization of living microorganisms. J Sol-Gel Sci Technol 342:211
7. Meunier CF, Dandoy P, Su B-L (2010) Encapsulation of cells within silica matrixes: towards a new advance in the conception of living hybrid materials. J Colloid Interface Sci 48:66–72
8. Premkumar JR, Lev O, Marks RS, Polyak B, Rosen R, Belkin S (2001) Antibody-based immobilization of bioluminescent bacterial sensor cells. Talanta 55(5):1029–1038
9. Perullini M, Rivero MM, Jobbagy M, Mentaberry A, Blimes SA (2007) Plant cell proliferation inside an inorganic host. J Biotechnol 127(3):542–548
10. Fiedler D, Hager U, Franke H, Soltmann U, Böttcher H (2007) Algae biocers: Astaxanthin formation in sol-gel immobilised living microalgae. J Mater Chem 17(3):261–266
11. Kuncova G, Podrazky O, Ripp S, Trögl J, Sayler GS, Demnerova K, Vankova R (2004) Monitoring of the viability of cells immobilized by sol–gel process. J Sol–Gel Sci Technol 31:1–8
12. Nguyen-Ngoc H, Durrieu C, Tran-Minh C (2009) Synchronous-scan fluorescence of algal cells for toxicity assessment of heavy metals and herbicides. Ecotoxicol Environ Saf 72:316–320
13. Sicard C, Perullini M, Spedalieri C, Coradin T, Brayner R, Livage J, Jobbagy M, Bilmes SA (2011) CeO2 nanoparticles for the protection of photosynthetic organisms immobilized in silica gels. Chem Mater 23(6):1374–1378
14. Perullini M, Jobbágy M, Bermúdez Moretti M, Correa García S, Bilmes SA (2008) Optimizing silica encapsulation of living cells: in situ evaluation of cellular stress. Chem Mater 20:3015–3018
15. Brumberger H (ed) (1993) Modern aspects of small-angle scattering.In: Proceedings of the NATO advanced study institutes, Como, Italy
16. Schmidt PW, Höhr A, Neumann H-B, Kaiser H, Avnir D, Lin JS (1989) Small angle X-ray scattering study of the fractal morphology of porous silicas. J Chem Phys 90(9):5016–5023
17. Vollet DR, Donatti DA, Ibãez Ruiz A, De Vicente FS (2010) Dynamical scaling in fractal structures in the aggregation of tetraethoxysilane-derived sonogels. J Appl Cryst 43(5):949–954
18. Zarzycki J (1987) Fractal properties of gels. J Non-Cryst Solids 95–96(1):173–184
19. Schaefer DW, Keefer KD (1984) Fractal geometry of silica condensation polymers. Phys Rev Lett 53(14):1383–1386
20. Mandelbrot BB (1983) The fractal geometry of nature. Freeman, San Francisco

21. Kim S, Lee K-S, Zachariah MR, Lee D (2010) Three-dimensional off-lattice Monte Carlo simulations on a direct relation between experimental process parameters and fractal dimension of colloidal aggregates. J Colloid Interface Sci 344:353–361
22. Schaefer DW, Martin JE, Wiltzius P, Cannell DS (1984) Fractal geometry of colloidal aggregates. Phys Rev Lett 52(26): 2371–2374
23. Vollet DR, Donatti DA, Ibãez Ruiz A (2001) A SAXS study of kinetics of aggregation of TEOS-derived sonogels at different temperatures. J Non-Cryst Solids 288(1–3):81–87
24. Brinker CJ, Keefer KD, Schaefer DW, Assink RA, Kay BD, Ashley CS (1984) Sol gel transition in simple silicates. J Non-Cryst Solids 63:45–59
25. Strawbridge I, Craievich AF, James PF (1985) The effect of the H2O/TEOS ratio on the structure of gels derived by the acid catalysed hydrolysis of tetraethoxysilane. J Non-Cryst Solids 72:139–157
26. Himmel B, Gerberb T, Bürger H (1990) WAXS- and SAXS-investigations of structure formation in alcoholic SiO_2 solutions. J Non-Cryst Solids 119:1–13
27. Reichenauer G (2004) Thermal aging of silica gels in water. J Non-Cryst Solids 350:189–195
28. Bhatia RB, Brinker CJ, Gupta AK, Singh AK (2000) Aqueous sol-gel process for protein encapsulation. Chem Mater 12: 2434–2441
29. Coiffier A, Coradin T, Roux C, Bouvet O, Livage J (2001) Sol-gel encapsulation of bacteria: a comparison between alkoxide and aqueous routes. J Mater Chem 11:2039–2044
30. Nassif N, Roux C, Coradin T, Rager MN, Bouvet O, Livage J (2003) A sol-gel matrix to preserve the viability of encapsulated bacteria. Mater Chem 13:203–208
31. Gerberb T, Himmel B, Bürger H (1994) WAXS- and SAXS-investigations of structure formation of gels from sodium water glass. J Non-Cryst Solids 175:160–168
32. Perullini M, Amoura M, Roux C, Coradin T, Livage J, Japas ML, Jobbagy M, Bilmes SA (2011) Improving silica matrices for encapsulation of Escherichia coli using osmoprotectors. J Mater Chem 21:4546–4552
33. Ferrer ML, Del Monte F, Levy D (2002) A novel and simple alcohol-free sol-gel route for encapsulation of labile proteins. Chem Mater 14:3619–3621
34. Ferrer ML, Yuste L, Rojo F, Del Monte F (2003) Biocompatible sol-gel route for encapsulation of living bacteria in organically modified silica matrixes. Chem Mater 15:3614–3618
35. Ferrer ML, García-Carbajal ZY, Yuste L, Rojo F, Del Monte F (2006) Bacteria viability in sol–gel materials revisited: cryo-SEM as a suitable tool to study the structural integrity of encapsulated bacteria. Chem Mater 18:1458–1463
36. Cavalcanti LP, Torriani IL, Plivelic TS, Oliveira CLP, Kellermann G, Neuenschwander R (2004) Rev Sci Instrum 75:4541
37. http://kur.web.psi.ch/sans1/SANSSoft/sasfit.html
38. Vinogradova E, Moreno A, Lara VH, Bosch P (2003) Multifractal imaging and structural investigation of silica hydrogels and aerogels. Silicon Chem 2:247–254
39. Vinogradova E, Moreno A, Lara VH, Bosch P (2003) Multifractal imaging and structural investigation of silica hydrogels and aerogels. Silicon Chem 2:247–254
40. Avnir D, Biham O, Lidar D, Malcai O (1998) Is the geometry of nature fractal? Science 279:39–40
41. Sorensen CM, Wang GM (1999) Size distribution effect on the power law regime of the structure factor of fractal aggregates. Phys Rev E 60(6):7143–7148
42. Knoblich B, Gerber T (2001) Aggregation in SiO_2 sols from sodium silicate solutions. J Non Cryst Solids 283:109–113
43. Boukari H, Harris MT (1997) Small-angle X-ray scattering study of the formation of colloidal silica particles from alkoxides: primary particles or not? J Colloid Interface Sci 194:311–318
44. Knoblich B, Gerber T (2001) The arrangement of fractal clusters dependent on the pH value in silica gels from sodium silicate solutions. J Non Cryst Solids 296:81–87
45. Beelen TPM, Wijnen PWJG, Vonk CG, Van Santen RA (1989) Catal Lett 3:209
46. Bohren CG, Huffmann DF (1983) Absorption and scattering of light by small particles. Wiley, New York